Journal of Membrane Science & Research

journal homepage: www.msrjournal.com

Research Paper

Synthesis and Characterization of Cation Exchange PVA-g-PAA/PBI sulfone Membrane for the Electrolysis of Sodium Chloride

Sandhya Pal, Savita Dixit, Sunder Lal

Maulana Azad National Institute of Technology Bhopal (Madhya Pradesh) 462003, India

ARTICLE INFO

Received 2015-10-05
Revised 2016-01-05
Accepted 2016-01-24
Available online 2016-01-24

KEYWORDS

Membrane electrolysis
Cation exchange membrane
PVA-g-PAA/PBI
Sodium hydroxide
Polymer membrane

GRAPHICAL ABSTRACT

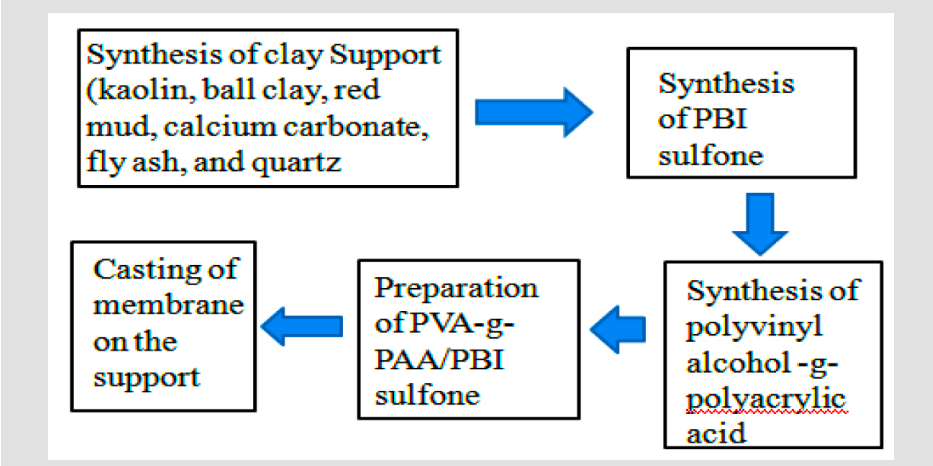

HIGHLIGHTS

- Different aspects of modification of PVA-g-PAA membrane by PBI sulphone
- Comparing the unmodified and modified membrane by the different characteristic properties
- Performance of the cation exchange membrane in the electrolysis of sodium chloride solution

ABSTRACT

The reported work is on the preparation and characterization of polyvinyl alcohol -g- Polyacrylic acid (PVA-g-PAA)/ Polybenzimidazole sulfone (PBIs) cation exchange membrane used for the electro dialysis of sodium chloride solution. The polymer syrup has been prepared using the grafting method with the help of polyvinyl alcohol and polyacrylic acid in the presence of water solvent. The polymer syrup is casted on a porous ceramic support to prepare a non-interpenetrating graft membrane in order to provide the sufficient mechanical strength. The composite membrane is modified by the PBI sulfone to introduce sulfonate charges on its surface. The prepared membrane is specific to the transport of sodium (Na^+) ions through its pores as by the migration mechanism. The modification effect is confirmed by SEM, FTIR, water uptake capacity, contact angle measurement, ion exchange capacity and current- voltage curve for the requirement of limiting current density. The electrolysis results of sodium chloride solution were reported in terms of current efficiency and energy consumption for sodium hydroxide production. The various operating parameters like salt concentration, current density, and circulation rates have an effect on the current efficiency which has been studied. It was observed that with an increase in salt concentration and flow rate, the current efficiency increased significantly. The maximum current efficiency which was obtained is 95.2% and the corresponding power consumption is 0.1224 kWh/ mol at 2N salt concentration and current density of 254 A/m^2.

1. Introduction

Electrolysis is used to transport salt ions from one solution through ion-exchange membranes to another solution under the influence of an applied electric potential difference. The major application of electrolysis has been used for the desalination of brackish water or seawater, treatment of industrial waste materials, recovery of useful materials from industrial effluents and salt production. The basic principles and applications of electrolysis were reviewed in the literature [1-5].

Electrolysis is a well known separation process, in which electrically charged membranes are used when the electrical potential difference is applied and chemical reaction takes place at the electrodes and separate ionic species [6]. Other applications of the electrolysis process includes production

* Corresponding author at: Phone: +91-755-4051653, fax: +91-755- 2670562
E-mail address: savitadixit1@yahoo.com (S. Dixit)

of caustic soda [7, 8], ultra pure water [9] and metal ion removal from waste water [10]. Electrolysis is used for the separation of brine in the presence of calcium sulfate (cation and anion exchange membranes) by using commercially available membranes (Asahi Glass membranes having current efficiency of 85% and power consumption varying between 2 and 7.1 kWh/m3) [11, 12]. In the coal-mine desalination brine (membranes from Asahi Glass yielding 85% recovery and energy consumption of 7.8–14.4 kWh/m^3) [13], removal of copper ions (cation and anion exchange membrane from Asahi Glass membranes, current efficiency 94.94% and power consumption 0.4 kWh/m^3) [4], lead ions (AR204SXR412 and CR67, MK111, Ionics, USA) [5] and Cr(III) and Cr(VI) ions (using Neosepta cation exchange membranes and Tokoyuma Soda anion exchange membranes) have a current efficiency of 80% [14] from waste water.

Electrolysis can be taken in two methods, one is the three-compartment cell which has cation and anion exchange membranes simultaneously and the second is the two compartment cell that has only one type of ion exchange membrane. Figure 1 shows a schematic diagram of the electrolysis of sodium chloride in a two-compartment cell having a cation exchange membrane.

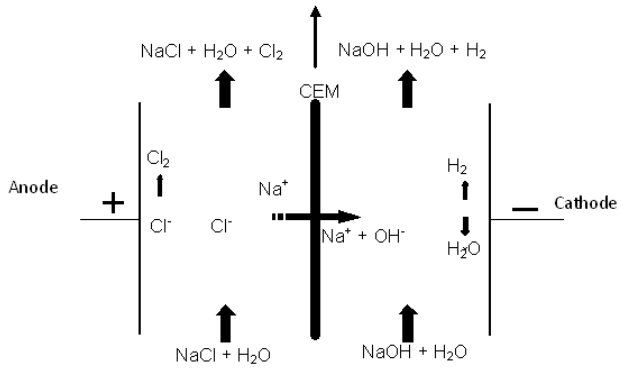

Fig. 1. Schematic diagram of membrane electrolytic cell using a cation-exchange membrane.

Two-compartment electrolysis cation exchange membranes have been used for various applications like fuel cells, super capacitors, batteries, sensors, chlor alkali cells and electro dialyzers [15-20]. The applications of electrodialytic are desalination of water, production of acids and bases, production of organic acids, recovery of metal ions, desalination of cheese whey [21-26], etc.

Electrolysis of NaCl at anode:

$$2Cl^- \rightarrow Cl_2 + 2e^-$$

Electrolysis of water at cathode:

$$2H_2O + 2e^- \rightarrow H_2 + 2OH^-$$

Overall Reaction:

$$2NaCl + 2H_2O \rightarrow Cl_2 + H_2 + 2NaOH \quad (1)$$

The charged membranes (in which functioned moieties are introduced in the polymer) are used for electro dialysis such as Polystyrene, Polyphosphazene, PS-DVB, poly (arylene ether sulfone), Polybenzimidazoles etc. Nafion (Du Pont) [27] Aciplex, and Flemion membranes are commercially available and being ion exchange membranes, they generally suffer from the problems of fouling and degradation at high temperature, which reduce efficiency and life. To overcome these above problems, we used Polybenzimidazoles based on cation-exchange membranes in the place of commercially available membranes to overcome these problems.

In this work, a ceramic supported cross linked PVA-g-PAA/PBI sulfone membrane has been prepared, having a high charge density of sulfonate charges on its surface. Polybenzimidazoles (PBIs) [28-30] are high performance polymers due to their excellent thermal, mechanical and oxidation stability. The PBI is now being looked upon as a possible alternative to Nafion for membrane electrolytes in the separation process. PVA is a hydrophilic polymer because the stability of the material in the water is low. In an effort to improve the stability in the electrolysis applications, Acrylic acid (AA) is used to catalyze the membrane. The cross linking is achieved using acrylic acid (AA) which converts the polymer material into hydrophobic. The membranes could be a cation exchange membrane and they facilitate the movement of proton from the anolyte to the catholyte chambers [31, 32]. The PVA-g-PAA cation exchange membrane was modified by using PBIs because the PBI has a heterocyclic benzimidazole ring with an amphoteric character, which can be easily modified with strong acids (such as phosphoric acid and/or sulfuric acid) to be used as an ionic conductive membrane [33].

2. Experimental

2.1. Materials

Analytical grade Acrylic acid, N, N-dimethylacetamide (DMAc), Quartz, Calcium carbonate, ball clay, kaolin feldspar and isophthalic acid have been purchased from S.D. Fine Chemicals (Mumbai, India). Diaminobenzene, lithium chloride and polyvinyl alcohol (PVA) were purchased from Loba chemie (Mumbai, India). Reagent grade polyphosphoric acid, sulfuric acid and Tetraethylorthosilicate (TEOS) were purchased from Fluke Chemicals (GmbH, Germany).

2.2. Preparation of clay supports

Ceramic support is prepared by mixing clays of kaolin, ball clay, red mud, calcium carbonate, fly ash, and quartz in water according to the reference [34]. This is while we replaced the feldspar and pyrophyllite of the some industrial waste materials like red mud and fly ash [35].

A paste of all these clays was made in water and casted on a zeolite surface in the form of a circular disc using an aluminium ring of 80 mm internal diameter and 5 mm thickness. All supports were dried at three different temperatures, 50 °C, 150 °C, and 300 °C, for 24 h to provide the sufficient mechanical and chemical strength. Then supports were further calcined at 850 °C for 10 h to impart required hardness and porosity. The clay support must have pores which are connected continuously from the feed stream to the permeate stream, otherwise no permeation through the support is possible. Finally, to get smooth and flat ceramic discs with a diameter 65 mm and thickness of 3–4 mm, the supports were polished by using a silicon carbide abrasive paper. To enhance the stability of the ion exchange membranes in oxidizing and reducing atmospheres, the coated clay supports were dipped into a polymerized solution of TEOS. The TEOS was prepared by continuous stirring of TEOS with, HCl, and H_2O in the molar ratio of 1:0.04:2.29 at room temperature. Finally, the clay supports were calcined at 1000^0C for 6h [34].

2.3. Preparation of polymer syrup

2.3.1. Synthesis of PBI sulfone

Diaminobenzene (DABz) (3.115 g) and isophthalic acid (IPA) (4.018 g) were mixed with polyphosphoric acid (PPA) (60 g) and placed in a round-bottom flask equipped with a reflux condenser with an inlet for nitrogen. The mixture was heated to 190^0C for 20 h. The polymerized PBI powder was collected and then dissolved in N, N-dimethylacetamide (DMAc) to prepare 10 wt% of the PBI solution.

To increase the ionic conductivity, the PBI film was treated with 98 wt% sulfuric acid at room temperature for three days (sulfonated-PBI, PBIs membrane). This acid-treated PBI film was washed with ethanol and subsequently dried at 60^0C for 24 h (Figure 2 shows the reaction of PBIs synthesis) [33].

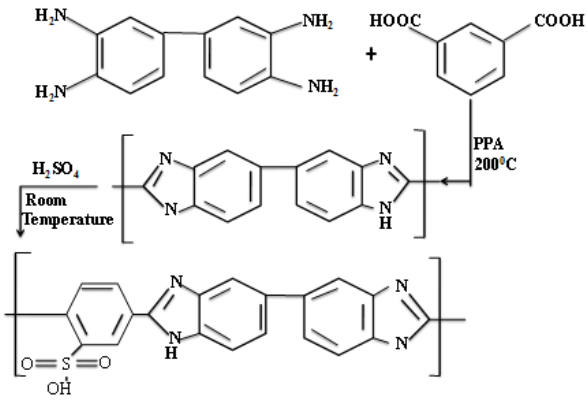

Fig. 2. The reaction of PBIs synthesis [33].

2.3.2. Synthesis of polyvinyl alcohol -g- polyacrylic acid (PVA-g-PAA)

10 g of polyvinyl alcohol (having a molecular weight of 1, 30,000 Dalton) was dissolved in water (90 ml) by stirring at 90 °C for 6 hours. Then acrylic acid (7.2 g, 0.1mol) was added to the mixture and the reaction was allowed to proceed at 80 °C for 5 hours [36, 37]. Figure 3 shows the structure of the PVA-g-PAA polymer chain.

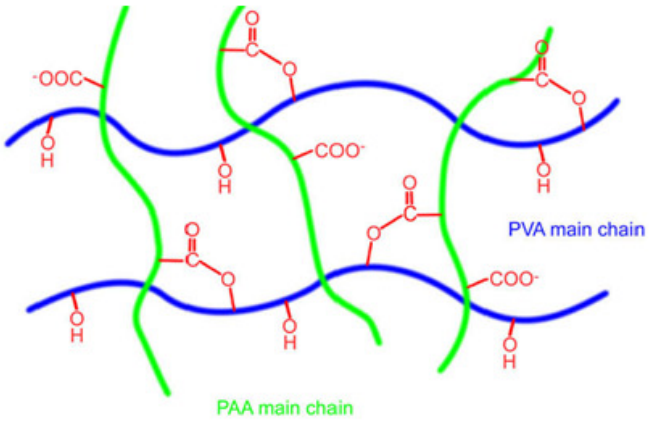

Fig. 3. Structure of PVA-g-PAA polymer chain.

2.4. Preparation of cation exchange polymer

2.4.1. Preparation of PVA-g-PAA/PBI sulfone

PBI sulfone (PBIs) (2 g) was dissolved in 50 ml of N, N'-dimethyl acetamide (DMAc) and heated at 120 °C for 5-6 hours. A minor amount of lithium chloride (typically 2%, 1 g) was also added to the solution in order to prevent the polymer from separating from the solution during storage for an extended period of time. The resulting solution was filtered to remove any undissolved polymer. This filtered solution of PBI sulfone (5 g) was added to 20 g of PVA-g-PAA solution and blended properly to make a homogeneous polymer syrup solution.

2.4.2. Casting of membrane on the support

The membrane on clay support was prepared as follows. The clay support was placed over the wet polyurethane foam and a thin, uniform layer of polymer syrup of approximately 1g was applied on the surface and is allowed to dry over it for 30 min.

The dipping of ceramic support in polyurethane foam (wet), was required in order to prevent the penetration of polymer in the pores of support. Then the polymer film was dried at room temperature for 8h, and thus the unreacted monomer was evaporated. The formed polymer composite membrane was kept in an oven for cross linking at 150 °C for two hours [34].

2.5. Characterization of membranes

2.5.1. FT-IR

The FTIR spectrum of the unmodified (PVA-g-PAA) and modified (PVA-g-PAA/PBIs) membranes was determined using a Perkin Elmer 1600 FTIR spectrometer to identify the functional groups introduced by the chemical modifications on the (PVA-g-PAA/PBIs) membrane in the range of 4000-400 cm^{-1}. The FT-IR fingerprint spectra of modified and un modified membranes were obtained by preparing a pellet of 1mg powder of crushed polymer films as samples and 200 mg of IR spectroscopic grade KBr pellets.

2.5.2. Scanning electron microscopy (SEM)

The FEI, Quanta 200HV spectrophotometer was used to study the structural morphology and asymmetric nature of the graft clay-composite membrane. The membrane samples were dipped in liquid nitrogen and modified with gold to a thickness of approximately 150 Å to create a conducting surface before being analyzed. This analysis has been carried out for both unmodified and modified membranes to observe the changes in structural morphology of the surfaces upon chemical modification.

2.5.3. Atomic force microscopy (AFM)

The Atomic force microscope is a high-resolution imaging characterization technique which has been applied extensively for studying ultra filtration and nano filtration membranes. AFM has eliminated the tedious process of sample preparation as it can image non-conducting samples and is used to determine the average pore size and surface roughness of the membrane. All the samples were scanned using Molecular Imaging (MI), USA made AFM equipment in Acoustic AC (AAC) mode. A sharp cantilever tip scans the surface of the membrane and generates a line profile of the surface. In conventional AFM, the contact mode is more commonly used for high-resolution imaging applied forces higher than ~300 pN. It is applied during the imaging of a soft membrane that typically distorts or damages the samples. This line profile is used to find the pore sizes, pore size distribution and also the surface roughness. The scan areas were 660× 660 and 1136× 1136 (A˚) 2, and the number of pixels per frame was 200× 200. The imaging rate was 10 frames/s.

2.5.4. Cation exchange capacity (CEC)

The cation exchange capacity is an important electrochemical property of an ion exchange membrane and is a measure of the number of fixed charges per unit weight of the dry membrane. In order to determine CEC, the modified film was first immersed in distilled water for a period of 24 h and then in 1M HCl aqueous solution for another 24 h to convert it to H^+ forms. The film was then washed with distilled water to remove excess acid. After that it was finally equilibrated with 0.5N NaOH aqueous solution for 24 h and the cation exchange capacity was determined from the reduction in alkalinity by back titration. The cation exchange capacity (CEC) was calculated from the following equation [37].

$$CEC = (N_1\text{-}N_2) * V/W \quad (2)$$

where N_1 is the normality of NaOH before equilibration, N_2 is the normality of NaOH after equilibration; V is the volume of NaOH taken for titration and W is the weight of modified PVA-g-PAA/PBIs film.

2.5.5. Contact angle measurement

The contact angle made by water on the PVA-g-PAA and PVA-g-PAA/PBIs membranes is measured by using Rame`-Hart Inc. (RHI) made Goniometer (model 100-00-230). The measurement of the contact angle helps in the estimation of the extent of the hydrophilic nature of the membrane.

2.5.6. Water uptake capacity

Water uptake measurement was performed by dipping the dried membranes (dried at 150 °C for 1 hour) in distilled water for 24 hours at room temperature. The membranes were taken out, wiped with blotting paper and then weighed. The water uptake capacity of the membrane was calculated by using the following equation:

$$\text{Water Uptake (\%)} = W_{wet} - W_{dry} * 100/W_{dry} \quad (3)$$

2.5.7. Thermo gravimetric analysis (TGA)

Thermo gravimetric analysis of the samples have been obtained using Perkin-Elmer Pyris 1 Thermal Analyzer to determine the thermal stability in the range of 50-800°C in air atmosphere at a heating rate of 10 °C min^{-1}.

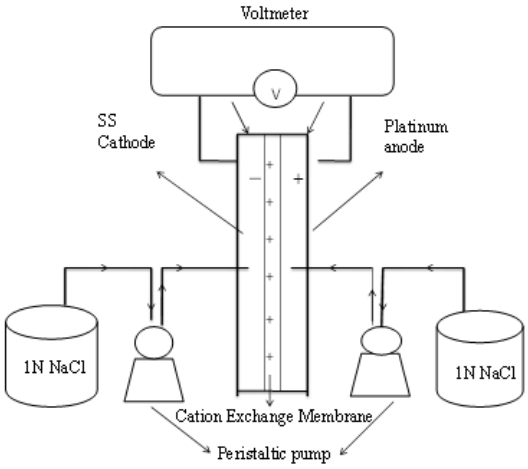

Fig. 4. Cell arrangement for measuring the potential drop across the membrane.

2.5.8. Current-Voltage characteristics

The current-voltage curve, which is an important characterization technique to determine the limiting current density of a membrane, was found out by using a test cell as shown in Figure 4. This cell consists of two

compartments arranged between Platinum anode and SS cathode with membrane in the center. Before the actual experiment, both the compartments were filled with 1N salt solution and circulated using peristaltic pumps for two hours to reach an equilibrium state. Then the current-voltage curve was obtained by slowly increasing the current across the membrane in small intervals and noting the cell voltage after waiting for the current to reach a steady value [33, 34].

2.5.9. Experimental set up for electrolysis

The experimental setup used for Electrolysis using the membrane is shown in Figure 5. It has two detachable compartments, each having a volume of 75 ml with the provision for fixing a membrane between the compartments. The inlets are connected to peristaltic pumps for the continuous flow of the electrolytic solutions. Of the two electrodes used, namely the cathode is made of stainless steel and the anode is made of platinum wires. The two solutions of one anolyte (NaCl) and another catholyte (water) are circulated through two 1 litre glass reservoirs using peristaltic pumps. The solutions are continuously stirred with magnetic stirrers and the power is supplied using rectifier (DC power source 0–32V 10 A). A potential difference is applied across the electrodes and a constant current density through the membrane is maintained [34]. The catholyte solution is taken for every 30 min time interval and the concentrations of produced NaOH are measured by the volumetric titration method. The different operating conditions are applied in the dialysis process of sodium chloride and every electrodialyis run is performed for 180 min under the different operating conditions. For the evaluation of the energy requirement, the voltage is supposed to be constant between two consecutive readings. The current efficiency (%) and the energy consumed (kWh/mol NaOH produced) are determined by the following formulae:

- The current efficiency (%)

$$\eta = \frac{\Delta C \cdot v}{I \cdot \Delta t/F} \times 100 \quad (4)$$

- Energy consumption

$$E = \frac{V_{Avg} \cdot I \cdot t}{\Delta N \cdot 1000} \quad \text{kWh/mol of NaOH produced} \quad (5)$$

where ΔC is the change in concentration of NaOH (mol/l) at a time of Δt seconds, v is the volume of catholyte solution in litres, I is the current in amperes, F is the Faraday constant, V_{Avg} is the average cell voltage for each electrolysis run, and ΔN is the mole of NaOH produced during the electrolysis run for time t.

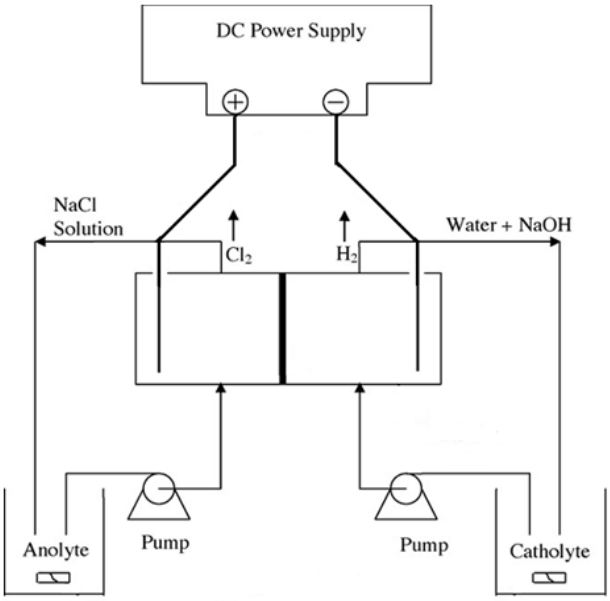

Fig. 5. Electro dialysis experimental setup.

3. Results and discussion

3.1. Fourier transform infrared spectroscopy

The FTIR spectrum of different membranes is obtained using Perkin Elmer 1600 FTIR spectrometer to identify the different functional groups present in the given material.

The FTIR spectra of the PVA-g-PAA and PVA-g-PAA/PBIs membranes are given (in the range of 4000-400cm^{-1}). Figure 6a depicts the FT–IR spectra of PVA-g-PAA. The fingerprint characteristic vibration bands of PVA-g-PAA appear at 1707 cm^{-1} n(C=O) and 1464 cm^{-1} n(C–O). The bands that correspond to the C–H stretching band of the methyl group (CH_3) are represented in the 2929 cm^{-1} range. Other bands at 1478 and 1384 cm^{-1} are associated with C–H asymmetric and symmetric stretching modes, respectively. The band at 3200 is associated with the O-H stretching of the acid group. The 1194 cm^{-1} band is assigned to the twist of the methylene group (CH_2), while C–C stretching bands are at 1054 and 784 cm^{-1}.

The FT-IR spectrum of the PVA-g-PAA/PBIs membrane is shown in Figure 6b. IR peaks (cm^{-1}) for stretching vibrations of the N-H group are shown by 3338 cm^{-1}, the C=N group by 1684 cm^{-1}, the C-N stretching by 743 cm^{-1}, and SO_2 by 1319 and 1151 cm^{-1}. The disappearance of C=O stretching vibration at 1684-1588 cm^{-1} suggests the nearly complete closure of the imidazole ring [33].

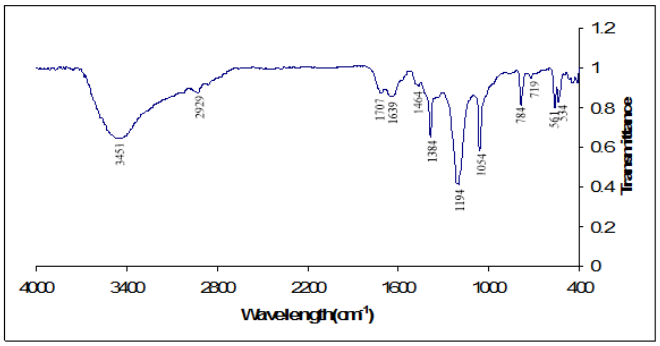

(a)

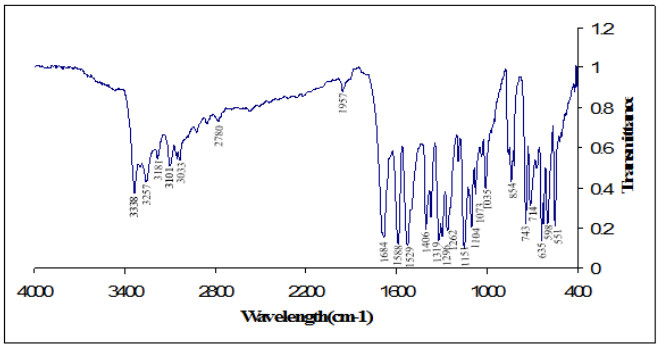

(b)

Fig. 6. FTIR spectra of (a) PVA-g-PAA membrane and (b) PVA-g-PAA/PBIs membrane.

3.2. Scanning electron microscopy

The SEM images of the top surface of the PVA-g-PAA and PVA-g-PAA/PBIs membrane at 10K and 15K magnification are shown in Figures 7a and b, respectively. Figure 7a shows the granular structure that clearly defines the polymerization of the monomer and the cluster phase of the polymer, overcoat of the white spots that define the grafting of two polymers. Figure 7b clearly shows the polymer chain. The dark region of the surface depicts the porous nature of the membrane. The depicted white shine spots scattered throughout the surface having light colour background showing the presence of the second phase most probably as PBI sulfone.

3.3. Atomic force microscopy

AFM images of PVA-g-PAA and PVA-g-PAA/PBIs membranes are shown in Figures 8a and b, respectively. We already observed that the dark and bright regions most likely represent pores and peaks in SEM images. The similar pores and peaks are also present in AFM images. In Figure 8a the pore size is comparatively smaller than Figure 8b. With this assumption, the average pore size of the PVA-g-PAA/PBIs determined as 50 nm. The pore

size determined from the AFM could be dead ends while the latter gives the average pore size of the conduits which connects both surfaces and takes the pore tortuosity of the membrane into account.

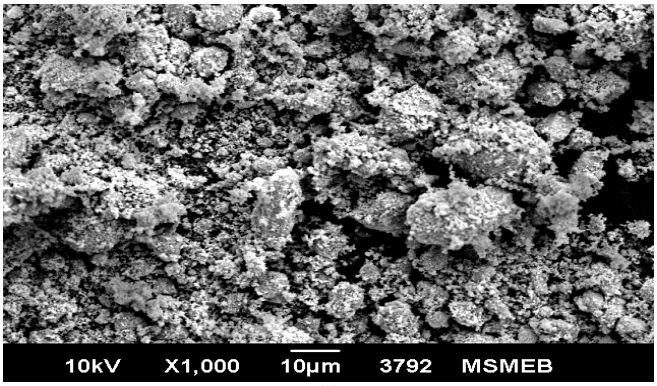

(a)

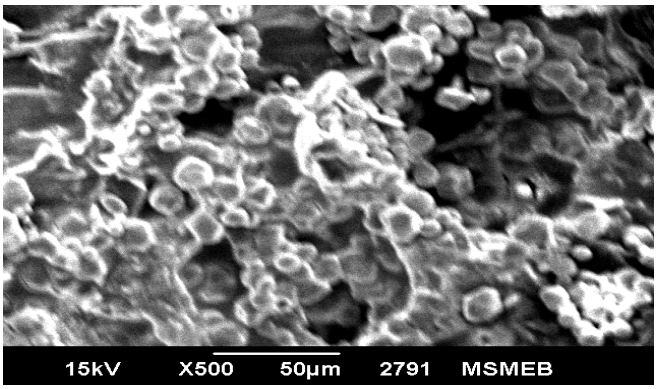

(b)

Fig. 7. SEM images of (a) PVA-g-PAA membrane and (b) PVA-g-PAA/PBI sulfone membrane.

3.4. Ion exchange capacity (IEC)

Ion-exchange capacity was calculated by using equation (2). Ion-exchange capacity for the PVA-g-PAA membrane is 2.8 and the PVA-g-PAA/PBIs membrane is 3.4mequiv/g. IEC of the PVA-g-PAA/PBIs membrane that will be high due to the presence of grafted sulphone copolymers.

3.5. Contact angle measurement

We have determined the contact angle of water with the PVA-g-PAA and PVA-g-PAA/PBIs membranes. The droplets of double distilled water (≈2 ml) are positioned at different places on the surface of the membrane, and a minimum of 20 readings are taken to find the average contact angle value.

The average contact angle for the PVA-g-PAA membrane was calculated to be 72° while the average contact angle for the PVA-g-PAA/PBIs membrane was 61° showing the PBI sulfone membrane to be more hydrophilic as compared to the PVA-g-PAA membrane.

3.6. Water uptake capacity

The water absorption capacity of the membrane impacts its dimensional stability, selectivity, electrical conductance and hydraulic permeability.

Water uptake capacity was calculated by using equation (3). According to the ASTM standard, the PVA-g-PAA membrane shows 10.5% and the PVA-g-PAA/PBIs membrane shows 13.75% water uptake capacity at room temperature. There are water molecules interacting with two imidazole rings and others are interacting with only one imidazole ring leading to an intermediate value between 2 and 4 positions of the water molecule. The literature suggested that N atom and N-H groups in PBI repeating units formed intermolecular hydrogen bonds in 2-4 positions of the water molecule [38]. These two pioneers observed the shifts of the N- H bond of PBI and carbonyl band of polyimide, which points to strong interactions and miscibility between these two polymers. The modified membrane has a high water uptake capacity but remains dimensionally stable as the membranes have been cross-linked during preparation and absorption of water that occurs at the sites of functional groups.

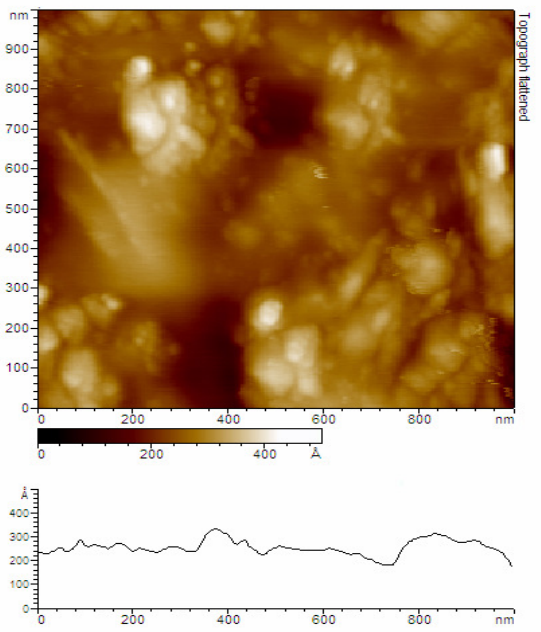

(a)

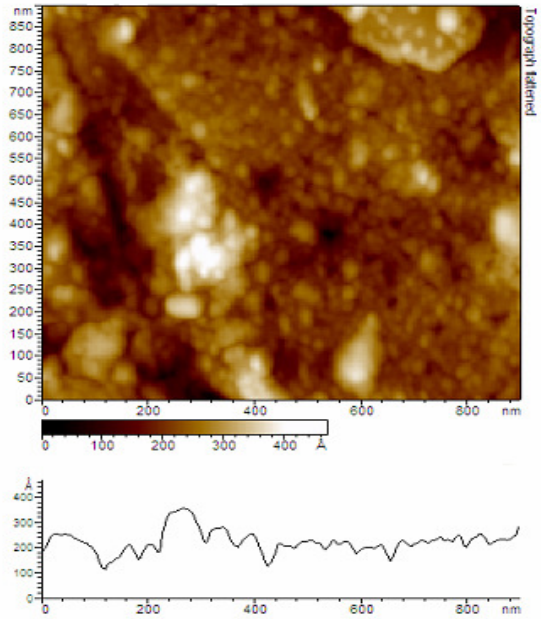

(b)

Fig. 8. AFM images of (a) PVA-g-PAA membrane and (b) PVA-g-PAA/PBI sulfone membrane.

3.7. TGA

Thermo gravimetric analysis was carried out in the range of 50-800 °C in air atmosphere at a heating rate of 10 °C min^{-1}. Figure 9 shows a comparison of the TGA curves obtained for (a) PVA-g-PAA/PBIs and PVA-g-PAA. The TGA curve of PVA-g-PAA/PBIs in Figure 9 shows a 5 % and 10 % weight losses up to 280 °C and 340 °C, respectively due to loss of both free and bound water molecules and further weight loss is due to degradation of the PBI sulfone by oxidation with air and we can observe from the TGA curve that the compound retains a residual weight of 20 % at 600 °C [39].

The TGA curve of PVA-g-PAA in Figure 9 shows a 5 % and 10 % weight loss up to 150 °C and 220 °C, respectively due to loss of both free and bound water molecules. Further weight loss is due to degradation of PVA-g-PAA by the oxidation with air and is completely disintegrated around 500 °C. The PVA-g-PAA/PBIs membrane degrades completely at 600 °C and denotes more stability in comparison to the PVA-g-PAA membrane.

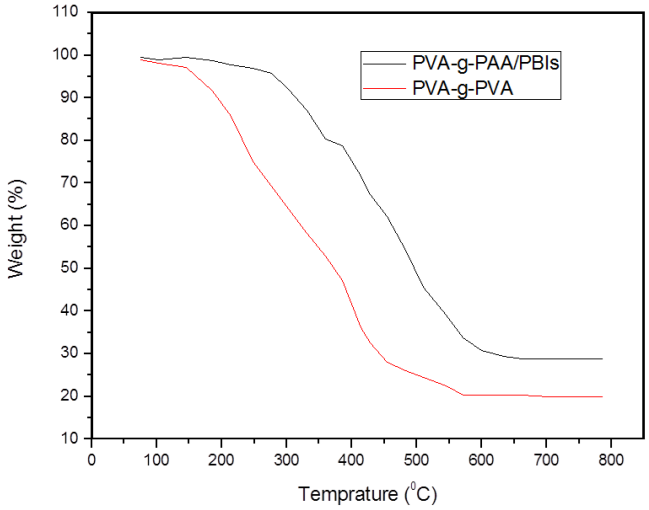

Fig. 9. TGA graph of PVA-g-PAA and PVA-g-PAA/PBIs.

3.8. Current–voltage characteristics

The current voltage characteristics of a membrane are obtained to find the limiting current density below which the membrane could successfully operate. It is seen that within the range of voltage applied, the voltage drop increases linearly with the applied current density, indicating Ohmic behaviour except that the straight line does not pass through the origin. The curves of different membranes (PVA-g-PAA and PVA-g-PAA/PBIs) are shown in Figures 10a and b, and it can be seen from the I-V curve, that there is first a linear segment, then followed by another very steep linear segment. The point at which the current shows the steady state behaviour (not fluctuation) with respect to voltage is the segment that defines the minimum current density. The first point where there is a change in the slope of the curve corresponds to the limiting current density and is found to be 505 A/m^2 at 0.5N and 410 A/m^2 at 1N for our membrane.

4. Effect of operating conditions on membrane performance

From the study and analysis of the modified and unmodified membranes, it is concluded that the PVA-g-PAA/PBIs membrane is a suitable cation exchange membrane because the PBIs are a more ionic conductive membrane with a modified surface of PVA-g-PAA for the cation (Na^+) to pass through them.

The performance of the membrane (PVA-g-PAA/PBIs) has been evaluated in terms of current efficiency and energy consumption for the production of sodium hydroxide. The current efficiency is a measure of the fraction of current carried by sodium ions through the cation exchange membrane. The operating parameters which affect the current efficiency and energy requirement are current density, salt concentration and flow rates of solutions. The effect of these parameters has been studied in order to determine the optimal conditions for operating at higher current efficiencies with lower energy consumption. When experiments were performed to determine influence of one parameter, the other variables were kept constant at standard conditions of 1N NaCl, 254.6 A/m^2 of current density and a circulation rate of 66 ml/min. At the base conditions, the current efficiency is found to be 92.3% and energy consumption of 0.1432 kWh/mol of NaOH is produced. In reference [40], it can be seen that the Nafion-117 membrane has a current efficiency of approx. 90%, and specific energy requirement is 0.1 kW/mol at 2N concentration of the salt, and 1000 A/m^2 current density when used for the electrolysis of sodium sulfate. The prepared membrane having the maximum efficiency of 95.2% and energy requirement is about 0.1224 kW/mol at the same concentration of salt at a current density of 254 A/m^2. The overall performance of the sulfone charged membrane including the current efficiency, cell voltage (average values), sodium ion transport number and energy consumption over a period of 90 min is given in Table 1.

4.1. Effect of current density on current efficiency and power requirements

The effect of current density is shown in Table 1. Figure 11 also shows the effect of current density over the current efficiency at standard conditions. It is observed that there is a slight increase in current efficiency up to 254 A/M^2 and it further decreases at higher current densities. The same was reported earlier by [34] where it has been indicated that the electro dialysis at higher current densities might have been performed above the limiting current. Thus, when operated above the limiting current density, the concentration polarization will come into picture reducing the current efficiency. At lower current density, i.e. at 127 A/M^2, there is a decrease in power consumption, but efficiency is low.

At the base conditions of 1N NaCl, 254 A/m^2 and at a circulation rate of 66 ml/min, the current efficiency is found to be 90.2% and the energy consumption of 0.4631kWh/mol of NaOH is produced.

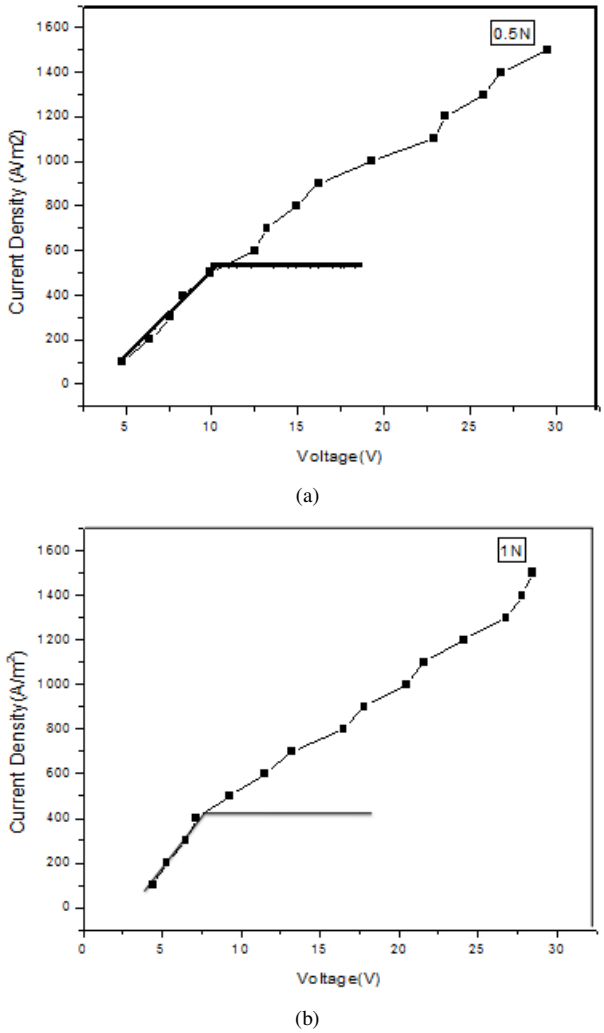

Fig. 10. (a) I–V characteristics of (a) PVA-g-PAA and (b) PVA-g-PAA/PBI sulfone cation exchange membranes.

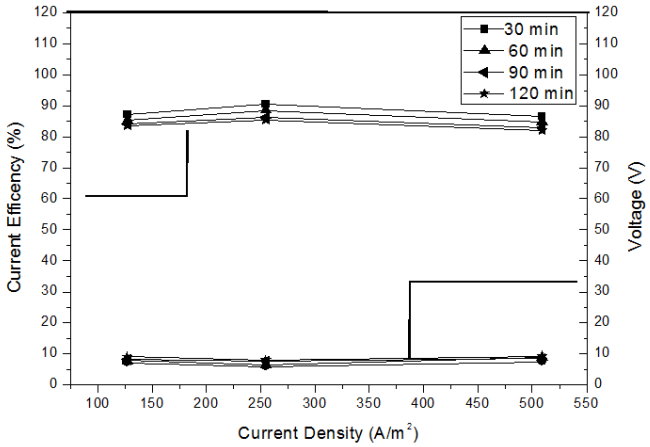

Fig. 11. Variation of current efficiency of CEM with time at different current densities (salt concentration = 1N, flow rate = 66 ml/min, temperature = 25 °C).

Table 1
Overall performance of the cation exchange membrane.

S.No.	Flow Rate (ml/min)	Time (min)	Current Density (A/m^2)	Conc. of NaCl (N)	Cell Voltage (V)	Current Efficiency (%)	Na^+ Transport number	Energy Consumption (KWh/mol)
1	33	30	127	0.5	5.6	88.7	0.887	0.6593
2	66	30	254	1.0	5.2	90.2	0.902	0.4631
3	99	60	509	2.0	5.2	89.6	0.896	0.1889
4	66	60	254	1.0	4.9	92.3	0.923	0.1432
5	99	90	509	1.0	6.9	87.6	0.876	0.6482
6	99	30	254	2.0	4.5	93.4	0.934	0.1376
7	99	60	254	2.0	3.8	95.2	0.952	0.1224
8	99	90	509	2.0	6.5	86.8	0.868	0.7434

4.2. Effect of salt (anolyte) concentration on current efficiency and power consumption

The effect of salt concentration on current efficiency, and power consumption is shown in Table 1. In Figure 12, the effect of the salt concentrations over the current efficiency has been found that the current efficiency was increasing with an increase in salt concentration and this behaviour is in perfect agreement with reports in the literature [34]. Thus, because of the higher current efficiency, it would be ideal to operate the electro dialysis process at higher concentrations, but this also has an associated disadvantage with it as discussed now. It was noticed that when the experiments were run at very high concentrations, the fouling of the membrane takes place. This reduces the current efficiency and increases the energy consumption. Thus, 0.5N, 1N and 2N concentrations of NaCl were used to study their effect on the current efficiency. The power consumption also followed a similar trend like the current efficiency. At higher concentrations of NaCl up to 2N, there is a decrease in power consumption, but eventually increases as the concentration is further increased.

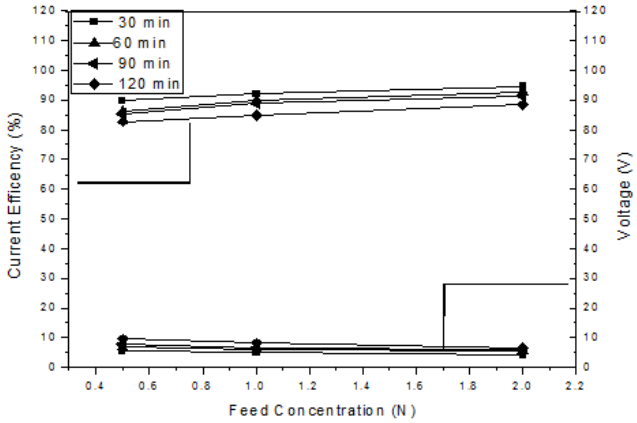

Fig. 12. Variation of current efficiency of CEM with time in different salt concentrations current density = 254 A/m^2, flow rate = 66 ml/min, temperature = 25 °C).

4.3. Effect of circulation rate on current efficiency and power consumption

The effect on the circulation rates of the catholyte and anolyte on current efficiency for CEM is shown in Figure 13. If the circulation rate increases, then the current efficiency will be increased, and this is proven by Figure 13. This may have been due to the transport behaviour associated with gas evolution that is not the rate limiting step in the narrow cell channel at the lower flow rates. The current efficiency is slightly high at lower flow rates, which can be explained because of the good mass transport behaviour associated with the gas evolution in the narrow cell channel. The trend of power consumption also follows the same trend as the current efficiency. The power consumption decreased with an increase in the circulation rates up to 66 ml/min, and then again increased further with a higher flow rate of 99 ml/min [34].

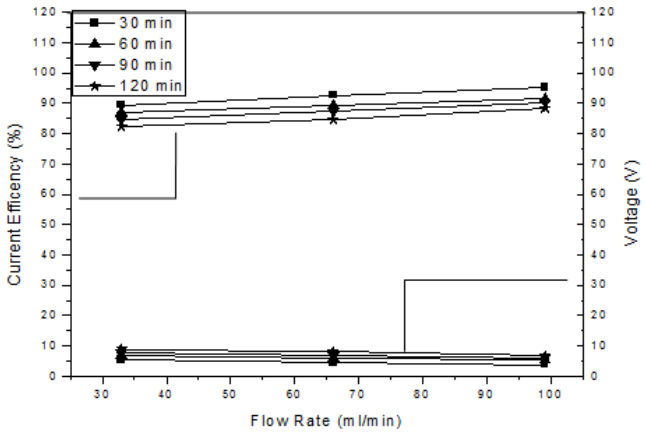

Fig. 13. Variation of current efficiency of CEM with time at different circulation rates (Current density = 254 A/m^2, salt concentration = 1N, temperature = 25 °C).

5. Conclusions

An ultra filtration, cross linked PVA-g-PAA/PBIs clay composite cation exchange membrane has been successfully prepared by chemically modifying a step by step process. This composite membrane has been prepared by first preparing the polymer syrup of PVA-g-PAA/PBIs using a multistep process with the help of a cross linking agent. The membrane prepared was thus homogeneously charged by PBIs reaction and found the comparative result of unmodified (PVA-g-PAA) and modified (PVA-g-PAA/PBIs) membranes. Prior to the membrane casting, the support was dipped in TEOS (tetraethoxysilane) and was found to withstand longer runs of experimentations without collapsing. The cation exchange membrane, thus prepared was characterized by scanning electron microscopy (SEM), FTIR spectroscopy, water content, contact angle measurement, atomic force microscopy (AFM) and cation exchange capacity. Finally, the membrane has been tested for at least for six months and we could get similar results within 8% of variation of that reported here.

The working efficiency of the modified (sulfone charged) membrane has been determined in terms of current efficiency, and power requirement with the effect of different operating conditions like current density, concentration of the solute, and circulation rate on these has been evaluated. The maximum current efficiency and the power consumption are found to be 95.2% and 0.1224 kWh/mol, respectively. The working efficiency of the membranes has been compared to the commercially available membranes (Nafion and Pall R 1030 membranes) and it was found that we have obtained an average current efficiency of about 87% and a power requirement of about 0.648 kWh/mol, which are more than that of the Nafion membrane (71.9%, 0.166 kWh/mol) and Pall R 1030 membrane (80– 62%) at almost similar operating conditions (509 A/m2, 2.5 M). The recent advances in the development of the cation-exchange membrane may encourage the suitability of these membranes for different types of electro-membrane applications.

6. References

[1] T. Chakrabarty, A. Michael Rajesh, A. Jasti, A.K. Thakur, A.K. Singh, S. Prakash,V. Kulshrestha, V.K. Shahi, Stable ion-exchange membranes for water desalination by electrodialysis, Desalination 282 (2011) 2–8.
[2] M. Sadrzadeh, T. Mohammadi, Treatment of sea water using electrodialysis: current efficiency evaluation, Desalination 249 (2009) 279-285.
[3] T. Mohammadi, A. Kaviani, Water shortage and sea water Desalination by lectrodialysis, Desalination 158 (2003) 267-270.
[4] T. Mohammadi, A. Moheb, M. Sadrzadeh, A. Razmi, Sepration of copper ion by electro- dialysis using taguchi experimental design, Desalination 169 (2004) 21-31.

[5] T. Mohammadi, A. Razmi, M. Sadrzadeh, Effect of operating parameters on $Pb2^{+}$ separation from waste water using electrodialysis, Desalination 167 (2004) 379-385.
[6] A.K. James, Riegel's 2003 handbook of industrial chemistry, 10th ed., Kluwer Academic/Plenum publications, NY, pp. 442-456.
[7] J.M. Ortiz, J.A. Sotoca, E. Exposito, F. Gallud, V.G. Garcia, V. Montiel, A. Aldaz, Brackish water desalination by electrodialysis: batch recirculation operation modelling, J. Membr. Sci. 252 (2005) 65–75.
[8] F. Faverjon, G. Durand, M. Rakib, Regeneration of hydrochloric acid and sodium hydroxide from purified sodium chloride by membrane electrolysis using a hydrogen diffusion anode-membrane assembly, J. Membr. Sci. 284 (2006) 323-330.
[9] R.K. Nagarale, G.S. Gohil, V.K. Shahi, Recent developments on ion-exchange membranes and electro-membrane processes, Adv. Colloid Interface Sci. 119 (2006) 97-130.
[10] M.I. Ahmed, H.T. Chang, J.R. Selman, T.M. Holsen, Electrochemical chromic acid regeneration process: fitting of membrane transport properties, J. Membr. Sci. 197 (2002) 63-74.
[11] E. Korngold, L. Aronov, N. Belayev, K. Kock, Electrodialysis with brine solution oversaturated with calcium sulfat, Desalination 172 (2005) 63-75.
[12] L. Bazinet, M.A. Farias, Effect of calcium and carbonate concentrations on cationic membrane fouling during electrodialysis, J. Colloid Interface Sci. 281 (2005) 188-196.
[13] T. Marian, Electrodialytic desalination and concentration of coal mine brine, Desalination, 162 (2004) 355-359.
[14] A. Tor, T. Buyukerkek, Y. Cengeloglu, M. Ersoz, Simultaneous recovery of Cr (III) and Cr(VI) from the aqueous phase with ion-exchange membrane, Desalination 171 (2004) 233-241
[15] V. Neburchilov, J. Martin, H. Wang, J. Zhang, A review of polymer electrolyte membranes for direct methanol fuel cells, J. Power Sources 169 (2007) 221-238.
[16] P. Sivaraman, S.K. Rath, V.R. Hande, A.P. Thakur, A.B. Samui, All-solid-supercapacitor based on polyaniline and sulfonated polymers, Synth. Met. 156 (2006) 1057-1064.
[17] E.L. Dewi, K. Oyaizu, H. Nishide, E. Tsuchida, Cationic polysulfonium membrane as separator in zinc–air cell, J. Power Sources 115 (2003) 149-152.
[18] K. Shimanoe, K. Goto, K. Obata, S. Nakata, G. Sakai, N. Yamazoe, Development of FET-type CO sensor operative at room temperature, Sens..Actuators B 102 (2004) 14-19.
Actuators B 102 (2004) 14-19.
[19] J. Balster, D.F. Stamatialis, M. Wessling, Electro-catalytic membrane reactors and the development of bipolar membrane technology, Chem. Eng. Process 43 (2004) 1115-1127.
[20] M.Y. Kariduraganavar, R.K. Nagarale, A.A. Kittur, S.S. Kulkarni, Ion Exchange Membrane: preparative method for electrodialysis and fuel cell application, Desalination 197 (2006) 225-246.
[21] S.A. Kalogirou, Seawater desalination using renewable energy sources, Prog. Energy Combust. Sci. 31 (2005) 242-281.
[22] X. Tongwen, Electrodialysis processes with bipolar membranes (EDBM) in environmental protection—a review, Resour. Conserv. Recycl. 37 (2002) 1-22.
[23] F. Faverjon, G. Durand, M. Rakib, Regeneration of hydrochloric acid and sodium hydroxide frompurified sodium chloride by membrane electrolysis using a hydrogen diffusion anode-membrane assem, J. Membr. Sci. 284 (2006) 323-330.
[24] C. Huang, T. Xu, Y. Zhang, Y. Xue, G. Chen, Application of electrodialysis to the production of organic acids:State-of-the-art and recent developments, J. Membr. Sci. 288 (2007) 1-12.
[25] V.E. Santarosa, F. Peretti, V. Caldart, J. Zoppas, M. Zeni, Study of ion-selective membranes from electrodialysis removal of industrial effluent metals II: Zn and Ni, Desalination 149 (2002) 389-391.
[26] L. Bazinet, Electrodialytic phenomena and their applications in the dairy Industry: a review, Crit. Rev. Food Sci. Nutr. 44 (2004) 525-554.
[27] L.M. Cormier, F. Ma, S.T. Bah, S. Guetre, M. Meunier, Sodium Salt-Splitting Performance of a Novel Ceramic-Polymer Composite Cation-Selective Membrane, J. Electrochem. Soc. 149 (2002) D21-D26.
[28] S. Qing, W. Huang, D. Yan, Synthesis and properties of soluble sulfonated polybenzimidazoles, React. Func. Polym. 66 (2006) 219-227.
[29] S. Qing, W. Huang, D. Yan, Synthesis and characterization of thermally stable sulfonated polybenzimidazoles obtained from 3,3′-disulfonyl-4,4′-dicarboxyldiphenylsulfone, J. Polym. Sci. A: Polym. Chem. 43 (2005) 4363-4372.
[30] F. Lufrano, V. Baglio, P. Staiti, A.S. Aricò, V. Antonucci, Development and characterization of sulfonated polysulfone membranes for direct methanol fuel cells, Desalination 199 (2006) 283-285.
[31] C.W. Lin, R. Thangamuthu, C.J. Yang, Proton-conducting membranes with high selectivity from phosphotungstic acid-doped poly(vinyl alcohol), J. Membr. Sci. 253 (2005) 23-31.
[32] S. Panero, P. Fiorenza, M.A. Navarra, J. Romanowska, B. Scrosati, Silica-Added, Composite Poly(vinyl alcohol) Membranes for Fuel Cell Application, J. Electrochem. Soc. 152 (2005) A2400-A2405.
[33] K. Hwang, J.H. Kim, S.Y. Kim, H. Byun, Preparation of Polybenzimidazole-Based Membranes and Their Potential Applications in the Fuel Cell System, Energies 7 (2014) 1721-1732.
[34] S. Savari, S. Sachdeva, A. Kumar, Electrolysis of sodium chloride using composite poly(styrene-co-divinylbenzene) cation exchange membranes, J. Membr. Sci. 310 (2008) 246-261.
[35] J. Yang, D. Zhang, J. Hou, B. He, B. Xiao, Preparation of glass-ceramics from red mud in the aluminium industries, Ceramic. Int. 34 (2008) 125-130.
[36] C.C. Yang, S.J. Chiu, k.T. Lee, W.C. Chien, C.T. Lin, C.A. Huang, Study of poly(vinyl alcohol)/titanium oxide compositepolymer membranes and their application on alkaline direct alcohol fuel cell, J. Power Sourc. 184 (2008) 44-51.
[37] C.W. Lin, R. Thangamuthu, C.J. Yang, Proton-conducting membranes with high selectivity from phosphotungstic acid-doped poly(vinyl alcohol) for DMFC applications, J. Membr. Sci. 253 (2005) 23-31.
[38] R.W. Kopitzke, C.A. Linkous, H.R. Anderson, G.L. Nelson, Conductivity and water uptake of aromatic-based proton exchange membranes electrolytes, J. Electrochem. Soc. 147 (2000) 1677-1681.
[39] J. Jouanneau, R. Mercier, L. Gonon, G. Gebel, Synthesis of sulfonated polybenzimidazoles from functionalized monomers: preparation of ionic conducting membranes, Macromolecules 40 (2007) 983-990.
[40] N. Tzanetakis, j.R. Varcoe, S. Slade, K. Scott, , Salt splitting with radiation grafted PVDF anion exchange membrane, Electrochem. Commun. 5 (2003) 115-119.